Revival of silenced echo and quantum memory for light

2011 New J. Phys. 13 093031

(http://iopscience.iop.org/1367-2630/13/9/093031)

New Journal of Physics
The open-access journal for physics

Revival of silenced echo and quantum memory for light

V Damon, M Bonarota, A Louchet-Chauvet, T Chanelière and J-L Le Gouët[1]

Laboratoire Aimé Cotton, CNRS-UPR 3321, Univ. Paris-Sud, Bât. 505, 91405 Orsay cedex, France
E-mail: jean-louis.legouet@lac.u-psud.fr

New Journal of Physics **13** (2011) 093031 (12pp)
Received 26 April 2011
Published 20 September 2011
Online at http://www.njp.org/
doi:10.1088/1367-2630/13/9/093031

Abstract. We propose an original quantum memory protocol. It belongs to the class of rephasing processes and is closely related to two-pulse photon echo. It is known that the strong population inversion produced by the rephasing pulse prevents the plain two-pulse photon echo from serving as a quantum memory scheme. Indeed, gain and spontaneous emission generate prohibitive noise. A second π-pulse can be used to simultaneously reverse the atomic phase and bring the atoms back into the ground state. Then a secondary echo is radiated from a non-inverted medium, avoiding contamination by gain and spontaneous emission noise. However, one must kill the primary echo, in order to preserve all the information for the secondary signal. In the present work, spatial phase mismatching is used to silence the standard two-pulse echo. An experimental demonstration is presented.

Contents

[1] Author to whom any correspondence should be addressed.

1. Introduction

The interaction of quantum light with an ensemble of atoms kindled intense research efforts in the past decade. The emblematic quantum memory challenge includes the conversion of a quantum state of light into an ensemble state of matter and the retrieval of a restored state of light. Light operates as a probe of the ensemble entangled state. Electromagnetically induced transparency (EIT) combined with the DLCZ generation of narrow-band heralded photons led to convincing experimental demonstrations in atomic vapors [1–3]. However, one cannot help but notice the small bandwidth offered by EIT-based protocols. Indeed, the spectrum of the incoming pulse of light has to fit the transparency window that is opened within the homogeneous width of the atomic transition. This practically limits the bandwidth to the megahertz range. To break this barrier, one may map the signal spectral components over the inhomogeneous width of the absorption line, according to the paradigm of the well-known photon echo scheme. In this context, solid state materials such as rare-earth ion-doped crystals (REIC) offer a prime alternative to atomic vapors since they combine the absence of motion with a long coherence lifetime and a large inhomogeneous width.

Although successful as a classical signal storage technique, photon echo does not work right away as a quantum memory procedure, as pointed out by several authors [4–6]. For instance, the two-pulse echo (2PE) suffers from the population inversion produced by the rephasing pulse. To efficiently reverse the phase of atomic coherences and get them phased together at a later time, this pulse has to simultaneously promote the atoms to the upper level of the optical transition. Working in a gain regime, detrimental to fidelity, the inverted medium also relaxes by spontaneous emission (SE), which further increases the intrinsic noise and makes this scheme inappropriate for the recovery of the initial quantum state of light. Last but not least, due to the spatial phase matching requirement, the 2PE signal propagates along the same direction as that of the driving fields. Hence, when composed of a few photons, the echo gets buried in the free induction decay (FID) long tail of the rephasing pulse [4].

To adapt the photon echo to quantum memory requirements, one has to get rid of massive population inversion. Original protocols such as the controlled reversible inhomogeneous broadening (CRIB) [7–10], the gradient echo memory (GEM) [11–16] and the atomic frequency comb (AFC) [17, 18] avoid population inversion. Either the phase reversal is produced by an external electric or magnetic field (CRIB and GEM) or rephasing just results from the initial preparation of the inhomogeneously broadened distribution (AFC). Those techniques have proved very successful in terms of efficiency [15, 19], multi-mode capacity [20, 21] and quantum fidelity [22, 23]. However, they all require a rather complex preparation step. In addition, by removing atoms from the absorption band, the preparation step reduces the intrinsic trapping capability of the medium.

In this paper, returning to 2PE basics, we propose an alternative approach, free from any preparation step. As already noted by Longdell [6, 24], the issue is population inversion and the resulting gain and SE noise, rather than the intense pulse in itself. A second intense pulse is able to bring the atoms back to the ground state, thus suppressing the undesired noise, and to simultaneously reverse the phase of the atoms, making them emit a secondary echo. The whole question is how to silence the primary 2PE and to preserve the integrity of the captured information until the emission of the secondary echo. Longdell [24] proposed to kill the primary echo by Stark-effect-induced interference [25, 26]. Here we propose to rely on spatial phase mismatching, which eliminates the need for an external field. This is explained in section 2,

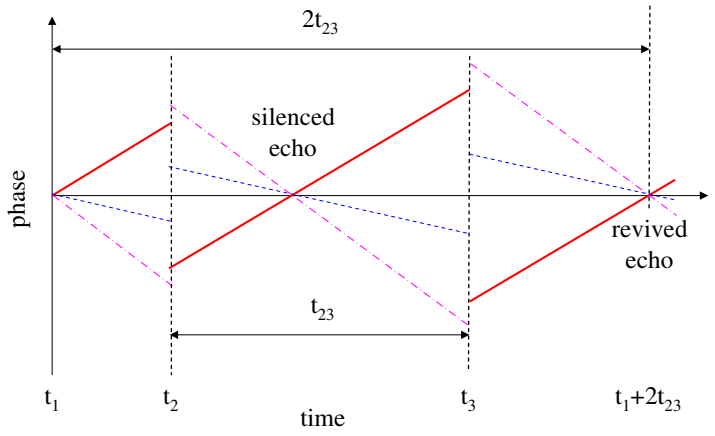

Figure 1. Revival Of Silenced Echo (ROSE). Excitation at time t_1 gives rise to atomic coherences. Departing from their initial common phase, the atomic coherences evolve at different rates, depending on their detuning from a reference. Rephasing pulses are shone at times t_2 and t_3. The atomic coherences get phased together at time $t_1 + 2t_{12}$ but the primary echo is silenced by spatial phase mismatching. The echo is revived at time $t_2 + 2t_{23}$.

where we describe the storage protocol. In section 3, we discuss rephasing the Bloch vectors with a pair of ARPs. Experimental results are presented in section 4.

2. Rephasing in the ground state with silenced primary echo

Let us consider a simple 2PE scheme, operating on an ensemble of two-level atoms. First a weak pulse, carrying the information to be stored, shines on the storage medium at time t_1. Then a strong pulse hits the medium at time t_2, rotating the Bloch vector by an angle of π. The π-rotation simultaneously reverses the inhomogeneous phase shift and promotes the atoms to the upper level. The atomic coherences get phased together again at time $t_e = t_1 + 2t_{12}$, where $t_{ij} = t_j - t_i$, and radiate an echo signal. The optical thickness must be large enough to allow for efficient capture of the initial signal pulse. In such a medium, population inversion by the rephasing pulse yields important gain and SE. Both phenomena affect the fidelity of the information recovery. To bring the atoms back to the ground state, one just has to apply a second π-pulse at time $t_3 > t_e$. As shown in figure 1, a secondary echo is then emitted at time $t'_e = t_1 + 2t_{23}$ from ground state atoms, free of gain and SE noise. However, this simple procedure only enables us to recover a part of the stored information. Another part has already been carried away by the primary echo at time t_e. To avoid this loss of information one has to silence the primary echo.

We rely on spatial phase mismatching to kill the primary echo. The pulses, directed along wavevectors $\vec{k}_1$ and $\vec{k}_2$, give rise to echo emission in the direction $\vec{k}_e = 2\vec{k}_2 - \vec{k}_1$, provided $k_e = |\vec{k}_e|$ is close to $k = |\vec{k}_1| = |\vec{k}_2|$. More precisely, the condition reads: $(k_e - k)L \ll \pi$, where L stands for the medium thickness. Indeed, the radiated field must match the spatial phase of the radiating atomic macroscopic polarization. If $(k_e - k)L > \pi$, no echo is emitted at time t_e but the macroscopic polarization does survive. The violation of the phase matching condition does not affect atomic coherences. The spectral phase shift is reversed anyway at time t_3 and, despite the absence of the primary echo, a secondary echo can be emitted at time

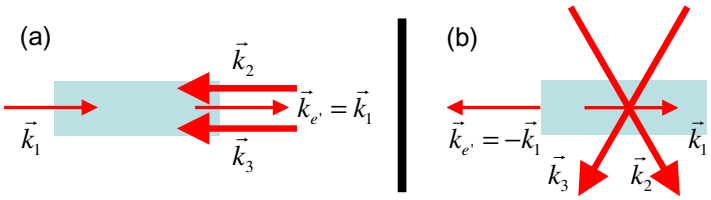

Figure 2. Beam configuration for signal recovery in the forward (a) and backward (b) directions. In (b), the rephasing pulses reach the medium (shaded area) from the sides.

$t'_e = t_1 + 2t_{23}$ provided $\vec{k}_{e'} = 2\vec{k}_3 - \vec{k}_e = \vec{k}_1 + 2(\vec{k}_3 - \vec{k}_2)$ satisfies the phase matching condition. If $\vec{k}_3 = \vec{k}_2$, emission takes place in the same $\vec{k}_1$ direction as the initial signal, whatever the common wavevector direction of the two rephasing pulses. This occurs, for instance, when the rephasing pulses counterpropagate with the incoming signal, a configuration that strictly forbids the 2PE emission. We coin this process Revival Of Silenced Echo (ROSE), believing that it may give a new start to photon echo in the quantum memory context.

Although three successive pulses are involved in the echo formation, the ROSE scheme strongly differs from what is usually called a 'three-pulse photon echo'. In the latter process, the atomic coherences resulting from interaction with the first pulse are converted into level population by the second pulse, and restored from population by the third pulse. Instead, all along the present echo process, the captured information is carried only by atomic coherences. The retrieval time of the echo lifts any ambiguity. It equals $t_1 + t_{23} + 2t_{12}$ in the conventional three-pulse echo, instead of $t_1 + 2t_{23}$ in the ROSE scheme.

The CRIB calculations [10] can be extended to ROSE quite directly. As in CRIB, the incoming signal pulse propagates through a spectrally uniform absorbing medium. Moreover, just as in CRIB, the signal is emitted when most atoms sit in the ground state. Hence, when $\vec{k}_3 = \vec{k}_2$, the recovery efficiency in the forward direction (see figure 2(a)) is expected to vary as $(\alpha L)^2\, e^{-\alpha L}$, where α stands for the absorption coefficient, and may reach a maximum value of 54% at $\alpha L = 2$, in the absence of coherence relaxation. When the T_2 finite duration of the optical coherence is taken into account, the echo intensity can be expressed as $(\alpha L)^2\, e^{-4t_{23}/T_2}$ times the transmitted intensity of the incoming signal, the latter itself being attenuated by the factor $e^{-\alpha L}$.

As in CRIB, a higher efficiency can be expected when the echo is recovered in the backward direction [7, 9, 10, 18]. This occurs when $(\vec{k}_1, \vec{k}_2) = (\vec{k}_2, \vec{k}_3) = \pi/3$, which leads to $\vec{k}_{e'} = -\vec{k}_1$ (see figure 2(b)). Since they illuminate the storage medium from the sides, the rephasing pulses penetrate a shorter distance and may undergo less propagation distortion. In the absence of coherence relaxation, the efficiency equals $(1 - e^{-\alpha L})^2$ and approaches 100% when $\alpha L \gg 1$.

As in CRIB [7, 9] or AFC [18, 27], two additional π-pulses may be used to convert the optical coherence into a ground state coherence and back, should a three-level Λ system be available. This way the storage time may be increased far beyond the optical coherence lifetime.

One may wonder whether the absence of primary echo really preserves the information mapping inside the medium. Indeed, when $(k_e - k)L > \pi$, the echo is killed but radiative emission remains in phase with atomic polarization over the distance $\pi/(k_e - k)$. Therefore, some information can creep in the medium over that coherence length. However, the mapping is not affected provided $\pi/(k_e - k)$ is much smaller than the α^{-1} characteristic distance.

The radiative migration is radically eliminated in counterpropagating configuration when $\vec{k}_2 = -\vec{k}_1$. Then the coherence length reduces to 1/3 wavelength. When the echo is recovered in the backward direction, with $(\vec{k}_1, \vec{k}_2) = \pi/3$, the coherence distance does not exceed one wavelength.

The ROSE scheme clearly disposes of two insurmountable faults of the conventional 2PE, namely the gain noise and the signal contamination by the FID tail of the rephasing pulses. Spontaneous emission (SE) properties deserve further consideration. During the time interval between the two rephasing pulses, atoms spontaneously decay to the ground state. Those atoms are promoted back to the upper level by the second strong pulse. Therefore, although most atoms sit in the ground state at the moment of the secondary echo, there remains some residual SE noise. In conventional 2PE, when the medium is totally inverted by the rephasing pulse, SE brings a noise of about 1 photon within the time slot and the solid angle of echo emission [4, 6]. After a second rephasing pulse, SE from the few atoms left in the upper level brings a small noise contribution to the retrieved signal. Should only 90% of the atoms be brought back to the ground state, this would still improve the signal-to-noise ratio by a factor of 10 with respect to the 2PE scheme. In addition to those incoherent features, SE is involved in coherent rephasing processes, as discussed in [6]. In the inverted medium, SE can play the role of the first pulse in a 2PE scheme, give rise to an echo after the second rephasing pulse and spoil the ROSE. However, according to the 2PE phase matching condition, the revived SE noise is radiated close to the direction $\vec{k}_3$, at large angular distance from the ROSE.

Finally, the ROSE scheme combines the absence of preparation step with broad-band capability. Unlike the protocols based on a preparation step, such as CRIB, GEM or AFC, the present process does not waste the available optical thickness. All the atoms initially present within the signal bandwidth may participate in the quantum memory. The main spectral width limitation may come from the rephasing pulses. The energy they have to exchange with the medium is indeed proportional to the operation bandwidth. Chirped control pulses offer an advantageous alternative to π-pulses in terms of bandwidth. In the next section we show that they can significantly improve the ROSE rephasing step.

3. Optimizing the rephasing step

In the previous discussion, phase reversal is assumed to be achieved by π-pulses. This may not be the best solution. First, since the spectral range of a π-pulse is determined by its inverse duration, the pulse energy grows quadratically with the spectral width. Broadband operation demands too much energy. Moreover, when propagating through a broadband absorber, a π-pulse converts most of its energy into atomic excitation. According to the numerical solution of the Maxwell–Bloch equations [28], 50% of a rectangular π-pulse is absorbed at depth $z = 1.78/\alpha$. As a consequence, the pulse undergoes strong distortions. Simultaneous energy loss and area conservation, as prescribed by the McCall and Hahn theorem [29], entail temporal stretching, which corresponds to the narrowing of the excited spectral interval as the pulse proceeds deeper and deeper into the medium.

Instead of flipping all the Bloch vectors simultaneously, one may rotate them sequentially with the help of chirped pulses, whose frequency is scanned at a rate r. Under the conditions of adiabatic rapid passage (ARP), the Bloch vector adiabatically follows the driving vector on the Bloch sphere and π-radian flipping can be achieved efficiently over the scanning range of the driving field. Unfortunately, a single ARP generally does not give rise to an echo.

Indeed, because atoms with different frequencies are excited successively, the Bloch vectors cannot be phased together at a later time. More precisely, a τ-long incoming signal cannot be recovered in the shape of a τ-long echo, except when the chirped pulse behaves as a brief excitation, interacting with all the atoms quite simultaneously. Since the scanning time of the initially excited spectral interval is given by $2\pi/(r\tau)$, simultaneous excitation of all the atoms by the ARP requires $2\pi/(r\tau) \ll \tau$, or $\phi \ll 1$ where the refocusing parameter is defined as $\phi = 2\pi/(r\tau^2)$. In this $\phi \ll 1$ situation, the ARP does not represent any improvement with respect to π-pulse excitation.

Although inaccessible to a single ARP in general, refocusing can be achieved by a *pair* of chirped pulses. Then the atomic coherences can be phased together, whatever the size of ϕ. In other words, a *pair* of ARPs is able to give rise to an echo even when the time needed by each ARP to scan the atom ensemble is much larger than the inverse spectral width of this ensemble [30].

The simplest ARP process is obtained by chirping the frequency of a field with a fixed amplitude at a constant rate. However, the field has to be switched on and off at large detunings from the atoms. Finite duration excitation gives rise to oscillatory features [31]. To flip the Bloch vector over a well-defined finite spectral interval, a complex hyperbolic secant (CHS) pulse is more appropriate [32]. High transfer efficiency has been reached over the targeted spectral band, while the atoms are left at rest outside [33, 34].

Frequency chirped pulses seem to be able to keep their properties during propagation through an absorbing material [35]. Specifically, they lose a much smaller fraction of energy than a π-pulse. To illustrate this property, let us consider a CHS pulse. The Rabi frequency and instantaneous frequency temporal variations are, respectively, defined by

$$\Omega(t) = \Omega_0 \,\mathrm{sech}(\beta(t - t_0)), \tag{1}$$

$$\omega(t) = \omega_0 + \mu\beta \tanh(\beta(t - t_0)). \tag{2}$$

According to equation (2), the field is chirped over a $2\mu\beta$-wide interval centered at ω_0. The chirp rate $\mathrm{d}\omega(t)/\mathrm{d}(t)$ reaches its maximum value $r_0 = \mu\beta^2$ at $t = t_0$. When the atoms are promoted to the upper level, the energy conveyed to the medium reads as

$$W_{\mathrm{at}} = 2\mu\beta A L n \hbar\omega_0, \tag{3}$$

where L, A and n, respectively, represent the medium length and cross-sectional area and the spectro-spatial atomic density. The incoming energy reads as

$$W_{\mathrm{in}} = \frac{1}{2} A c \epsilon_0 \int \mathrm{dt} |\Omega(t)\hbar/d|^2 = A c \epsilon_0 |\Omega_0 \hbar/d|^2/\beta, \tag{4}$$

where d represents the transition dipole moment. The fraction of incoming energy that is stored in the medium can be expressed in terms of the absorption coefficient $\alpha = \pi\omega_0 d^2 n/(c\hbar\epsilon_0)$ as

$$\frac{W_{\mathrm{at}}}{W_{\mathrm{in}}} = \frac{2}{\pi}\frac{r_0}{\Omega_0^2}\alpha L. \tag{5}$$

Since adiabatic passage precisely requires that $r_0/\Omega_0^2 \ll 1$ [33], the storage of a small fraction of energy in the medium can be made consistent with the adiabatic condition, whatever be the optical depth αL. As pointed out above, the strong distortion of a π-pulse propagating through an absorbing medium is connected with the loss of an important fraction of initial energy. Traveling through the same medium, a CHS pulse might undergo less distortion, in connection with a much lower energy loss, and preserve its initial properties much deeper into the medium.

4. Experimental

Experimentally we pursue a twofold objective. Firstly, we need to confirm the generation of the revived echo, with the expected efficiency, when the primary echo is silenced by spatial phase mismatching. We concentrate on the counterpropagating configuration (see figure 2(a)) where mismatching is maximum. The two rephasing pulses follow the same path, in an opposite direction to the signal field. Secondly, we want to verify that the second rephasing pulse actually brings the atoms back to the ground state.

A first experiment is conducted in a 0.5 at.% Tm^{3+} : YAG crystal operating at 793 nm. The sample is cooled down to 2.8 K in a variable temperature liquid helium cryostat. The counterpropagating light beams are split from a home-made, extended cavity, continuous wave, ultra-stable semi-conductor laser [36], featuring a stability better than 1 kHz over 10 ms. To manage the rephasing and signal paths separately, we make a small angle of $\approx 2^\circ$ between them. This way we not only extract the echo easily but also further reject reflections from the cryostat windows. Those precautions will prove essential in shot-noise limited measurements.

The signal beam waist is adjusted to 30 μm, with a rephasing beam 1.6 times bigger. All the fields are polarized along the [001] crystallographic axis [37]. In order to avoid propagation effects, we slightly detune the laser from the absorption line center to $\alpha L = 1.05$.

The rather high Tm^{3+} concentration reduces T_2 to less than 50 μs, making the ROSE wither fast. This impacts on the parameter accessible range. To simultaneously satisfy $T_2\beta \gg 1$ and $\mu\beta^2 \ll \Omega_0^2$ (adiabatic passage condition), one is led to the minimum $\mu = 2$ acceptable value, with $\beta/(2\pi) = 120$ kHz. Hence, population is inverted over a $\mu\beta/\pi = 480$ kHz-wide spectral interval.

With a rephasing pulse separation of $t_{23} = 13\,\mu$s, the storage time is equal to 26 μs. The 3.5 μs-long (full-width at half-maximum) incoming signal and the recovered ROSE are displayed in figure 3(a). Spatial-mode filtering through a single-mode fiber at the crystal output efficiently rejects stray light from the CHS rephasing pulses. Those pulses are monitored with a control detector, as shown in figure 3(b). As can be seen in this figure, we truncate CHS waveforms to $6\beta^{-1}$. The recovery efficiency of $\approx 10\%$ is consistent with the $(\alpha L)^2\, e^{-\alpha L - 4t_{23}/T_2}$ predicted value, setting $T_2 = 42\,\mu$s. The latter T_2 value agrees with independent measurements.

The refocusing parameter defined in section 3 reads as $\phi = 2\pi/(\mu\beta^2\tau^2)$. To accomodate the incoming pulse bandwidth, CHS parameters must satisfy $\mu\beta\tau > \pi$, which results in $\phi < 2\mu/\pi$. With $\mu = 2$, ϕ remains close to unity, thus allowing for some refocusing of the Bloch vectors after the first CHS pulse. It may be interesting to check that complete refocusing can be achieved by a pair of CHS, even when $\phi \gg 1$, i.e. when coherences cannot be phased together after a single CHS. These conditions are met in the next experiment.

We undertake the second experiment in a 0.005 at.% Er^{3+}:YSO, 7.5 mm-thick, crystal at 1.5 μm. This material offers attractively slow relaxation rates that allow time for the ROSE to bloom. The upper level decays in 10 ms and we have measured an optical coherence lifetime T_2 as large as 230 μs. To reach such a high T_2 value, one cools down the crystal to 2 K and one lifts the Kramers degeneracy with a magnetic field of ≈ 2.2 T. The light beams are directed along the b axis, perpendicular to the magnetic field. The crystal is birefringent and T_2 is optimized when the neutral lines D_1 and D_2 are oriented at 45° from the magnetic field [38]. In spite of its attractive T_2 figure, Er^{3+}:YSO exhibits some drawbacks with respect to Tm^{3+}:YAG. In YSO, the host matrix birefringence should affect side illumination in the configuration described in figure 2(b). Besides, in Er^{3+}:YSO one does not enjoy a Λ three-level system configuration as in

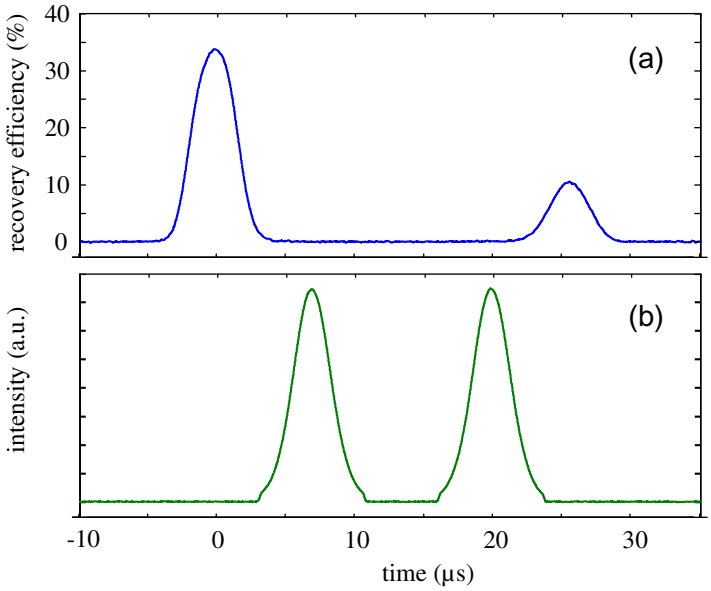

Figure 3. ROSE in Tm^{3+}:YAG. Opacity is adjusted to $\alpha L = 1.05$. The incoming pulse and the echo are displayed in (a). Counterpropagating with the CHS rephasing pulses, they are monitored with a control detector and represented in (b). In (a), efficiency refers to the intensity of the incoming signal, measured at the input side of the crystal.

Tm^{3+}:YAG, which is required for optical-to-spin coherence conversion (see [39] and references therein). Last but not least, single-photon detectors are more efficient at Tm^{3+}:YAG transition wavelength.

The light source is an erbium-doped fiber, distributed feedback, commercial laser (KOHERAS). This source features good stability, with a coherence time larger than 1ms and a jitter of a few kHz over 100 μs. The rephasing beam is 2.5 times bigger than the signal beam, whose beam waist is measured to be 45 μm at the crystal. All the fields are polarized along D_1. The opacity αL reaches $\approx$2 at the line center. The echo is extracted by a beam splitter and collected on a photodiode.

First we check the inversion efficiency of a CHS pulse with parameters $\beta = 125 \times 10^3\ s^{-1}$ and $\mu = 10$, corresponding to excitation over a 400 kHz-wide interval. As before, the CHS duration is limited to $6\beta^{-1}$. Slightly detuning the laser from the line center, we measure an opacity $\alpha L = 0.71$. A 3 μs-long (full-width at half-maximum) Gaussian-shaped signal pulse is shone through the crystal. We successively detect the transmitted profile before and after inversion by a counterpropagating CHS pulse (figure 4). The pulse sequence is repeated at 10 Hz rate. We observe an amplification factor of 3.55. Through a totally inverted medium, with an upper-level population $n_b = 1$, this factor should reach $e^{2\alpha L} = 4.13$. The measured factor corresponds to $n_b = \mathrm{Ln}(3.55)/(2\alpha L) = 0.89$.

With the same CHS parameter values, the same input signal duration and the same opacity, we check the ROSE process. In the experiment presented in figure 5, the rephasing pulse separation is adjusted to 41 μs, which leads to a storage time of 82 μs. The recovery efficiency, as measured with respect to the incoming pulse at the crystal input, reaches 12%, in excellent agreement with the $(\alpha L)^2\, e^{-\alpha L - 4t_{23}/T_2}$ expected value (see section 2). As shown in figure 5

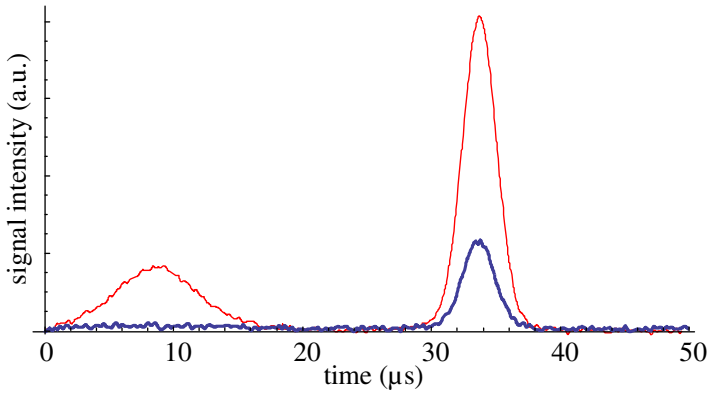

Figure 4. Population inversion by a CHS pulse. A probe pulse is detected before (thick blue line) and after (red thin line) excitation by a 400 kHz-wide CHS pulse. Some stray light from the cryostat windows reveals the CHS profile and time position.

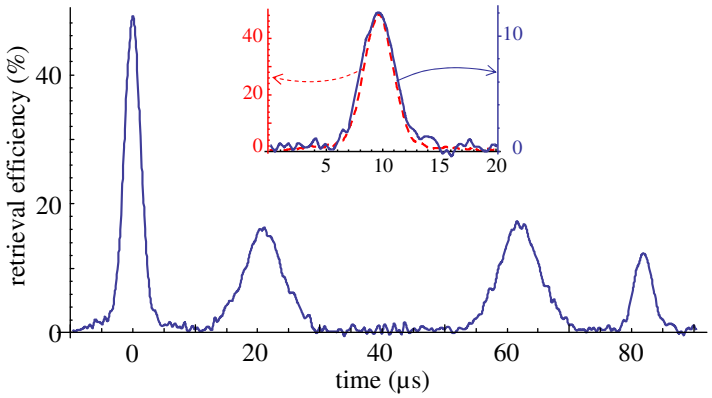

Figure 5. ROSE in Er^{3+}:YSO. After the arrival of a 3 μs-long weak pulse, two CHS pulses successively illuminate the crystal from the opposite direction. They cover a 0.4 MHz wide spectral interval. Their time separation is adjusted to 41 μs. Their time evolution is revealed by reflections from the cryostat windows. The echo is radiated 82 μs after the first pulse. The incoming signal (dashed line) and echo (solid line) temporal profiles are compared in the inset.

(inset), the temporal profile of the echo nearly coincides with that of the incoming pulse, showing that the CHS spectral range is correctly adjusted to the signal width. The refocusing parameter ϕ reaches $2\pi/(\mu\beta^2\tau^2) \approx 4.5$, attesting to the absence of Bloch vector refocusing after the first CHS pulse.

To check the CHS ability to bring ions back to the ground state, we probe the crystal transmission spectrum after illumination by one or two CHS pulses. In order to optimize the beam overlap, we slightly modify the setup. All the light fields now copropagate, being carried by a single beam. The detector is protected from the intense CHS pulses by an acousto-optic modulator operating as an optical switch. The transmitted light is detected through a pinhole that selects the uniformly excited central region of the crystal. The CHS pulses are defined by the same β and μ values as above. The Rabi frequency is adjusted to $\approx 3.5 \times 10^6\ s^{-1}$. The

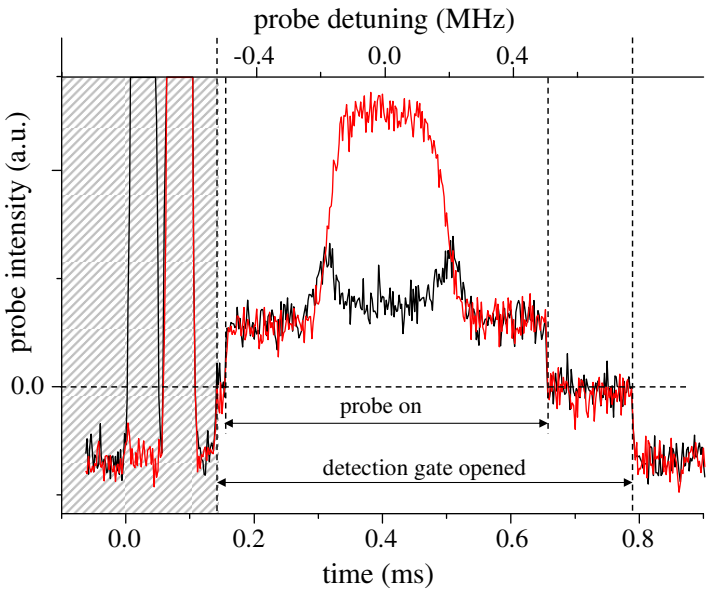

Figure 6. The transmission spectrum is probed after illumination by one (red line) or two (black line) CHS pulses. The probe pulse is scanned over 1 MHz in 0.5 ms. The upper level population reaches 0.7 after one CHS and drops to less than 0.1 after the second CHS. The opacity is adjusted to $\alpha L = 1.0$.

probe field is scanned over a 1 MHz-wide interval in 0.5 ms. The recorded spectra are displayed in figure 6. The inverted interval edges are not vertical. Instead they exhibit a finite width of $\approx$50 kHz, consistent with the computed value obtained with $\mu = 10$ and a finite pulse duration of $6\beta^{-1}$. The laser being tuned to $\alpha L = 1.0$, the upper-level population reaches 0.7 after one CHS and drops to less than 0.1 after the second CHS. As discussed in section 2, this should be enough to reduce the spontaneous emission noise by 10 with respect to the conventional 2PE scheme.

5. Conclusion

We have described an original ROSE scheme where an echo signal is radiated from ground state atoms with optimum efficiency. This process remedies the conventional photon echo drawbacks [4, 5, 24] in the prospect of quantum storage. In the small optical thickness regime, optimum recovery efficiency has been reached experimentally. Complex hyperbolic secant pulses, more robust to propagation than π-pulses, have proved efficient in rephasing the atomic coherences. With respect to previously proposed schemes such as CRIB and AFC, ROSE avoids complex and optical-depth consuming preparation steps while preserving the photon echo broadband and multimode capability.

The ROSE scheme can be extended to Raman excitation, in situations where the Raman transition may offer a large bandwidth, such as in a vapor, where non-collinear signal and coupling beams make the inhomogeneous broadening adjustable [40]. The primary echo can be killed by just switching off the coupling beam at the rephasing time. One needs two sublevels only in the ground state, instead of three as in [40].

Acknowledgments

We acknowledge stimulating and fruitful discussions with J J Longdell. This work was supported by the European Commission through the FP7 QuRep project, by the national grant ANR-09-BLAN-0333-03 and by the Direction Générale de l'Armement.

References

[1] Chanelière T, Matsukevich D, Jenkins S, Lan S, Kennedy T and Kuzmich A 2005 *Nature* **438** 833
[2] Eisaman M D, André A, Massou F, Fleischhauer M, Zibrov A and Lukin M D 2005 *Nature* **438** 837
[3] Appel J, Figueroa E, Korystov D, Lobino M and Lvovsky A I 2008 *Phys. Rev. Lett.* **100** 093602
[4] Ruggiero J, Le Gouët J L, Simon C and Chanelière T 2009 *Phys. Rev.* A **79** 053851
[5] Sangouard N, Simon C, Minář J V, Afzelius M, Chanelière T, Gisin N, Le Gouët J L, de Riedmatten H and Tittel W 2010 *Phys. Rev.* A **81** 062333
[6] Ledingham P M, Naylor W R, Longdell J J, Beavan S E and Sellars M J 2010 *Phys. Rev.* A **81** 012301
[7] Moiseev S A and Kröll S 2001 *Phys. Rev. Lett.* **87** 173601
[8] Nilsson M and Kröll S 2005 *Opt. Commun.* **247** 393
[9] Kraus B, Tittel W, Gisin N, Nilsson M, Kröll S and Cirac J I 2006 *Phys. Rev.* A **73** 020302
[10] Sangouard N, Simon C, Afzelius M and Gisin N 2007 *Phys. Rev.* A **75** 032327
[11] Alexander A L, Longdell J J, Sellars M J and Manson N B 2006 *Phys. Rev. Lett.* **96** 43602
[12] Hétet G, Longdell J J, Alexander A L, Lam P K and Sellars M J 2008 *Phys. Rev. Lett.* **100** 23601
[13] Hétet G, Longdell J J, Sellars M J, Lam P K and Buchler B C 2008 *Phys. Rev. Lett.* **101** 203601
[14] Longdell J J, Hétet G, Lam P K and Sellars M J 2008 *Phys. Rev.* A **78** 032337
[15] Hedges M P, Longdell J J, Li Y and Sellars M J 2010 *Nature* **465** 1052
[16] Lauritzen B, Minár J, de Riedmatten H, Afzelius M, Sangouard N, Simon C and Gisin N 2010 *Phys. Rev. Lett.* **104** 080502
[17] de Riedmatten H, Afzelius M, Staudt M U, Simon C and Gisin N 2008 *Nature* **456** 773
[18] Afzelius M, Simon C, de Riedmatten H and Gisin N 2009 *Phys. Rev.* A **79** 052329
[19] Bonarota M, Ruggiero J, Le Gouët J L and Chanelière T 2010 *Phys. Rev.* A **81** 033803
[20] Usmani I, Afzelius M, de Riedmatten H and Gisin N 2010 *Nat. Commun.* **1** 1
[21] Bonarota M, Le Gouët J L and Chanelière T 2011 *New J. Phys.* **13** 013013
[22] Saglamyurek E, Sinclair N, Jin J, Slater J A, Oblak D, Bussières F, George M, Ricken R, Sohler W and Tittel W 2011 *Nature* **469** 512
[23] Clausen C, Usmani I, Bussières F, Sangouard N, Afzelius M, de Riedmatten H and Gisin N 2011 *Nature* **469** 508
[24] McAuslan D, Ledingham P, Naylor W, Beavan S, Hedges M, Sellars M and Longdell J 2011 *Phys. Rev.* A **84** 022309
[25] Meixner A J, Jefferson C M and Macfarlane R M 1992 *Phys. Rev.* B **46** 5912
[26] Chanelière T *et al* 2008 *Phys. Rev.* B **77** 245127
[27] Afzelius M *et al* 2010 *Phys. Rev. Lett.* **104** 040503
[28] Ruggiero J, Chanelière T and Le Gouët J L 2010 *J. Opt. Soc. Am.* B **27** 32
[29] McCall S L and Hahn E L 1969 *Phys. Rev.* **183** 457
[30] Lauro R, Chanelière T and Le Gouët J L 2011 *Phys. Rev.* B **83** 035124
[31] Vitanov N V and Garraway B M 1996 *Phys. Rev.* A **53** 4288
[32] Roos I and Mølmer K 2004 *Phys. Rev.* A **69** 022321
[33] de Seze F, Dahes F, Crozatier V, Lorgeré I, Bretenaker F and Le Gouët J L 2005 *Eur. Phys. J.* D **33** 343
[34] Rippe L, Nilsson M, Kröll S, Klieber R and Suter D 2005 *Phys. Rev.* A **71** 062328
[35] Zafarullah I, Tian M, Chang T and Babbitt W R 2007 *J. Lumin.* **127** 158
[36] Crozatier V, de Seze F, Haals L, Bretenaker F, Lorgeré I and Le Gouët J L 2004 *Opt. Commun.* **241** 203

[37] Sun Y, Wang G M, Cone R L, Equall R W and Leask M J M 2000 *Phys. Rev.* B **62** 15443
[38] Böttger T 2002 Laser frequency stabilization to spectral hole burning frequency reference in erbium-doped crystals: material and device optimization *PhD Thesis* Montana State University, Bozeman, MT
[39] Louchet A, Le Du Y, Bretenaker F, Chanelière T, Goldfarb F, Lorgeré I, Le Gouët J-L, Guillot-Noël O and Goldner P 2008 *Phys. Rev.* B **77** 195110
[40] Le Gouët J-L and Berman P R 2009 *Phys. Rev.* A **80** 012320